JVI Journals.ASM.org

Characterization of the Determinants of NS2-3-Independent Virion Morphogenesis of Pestiviruses

O. Klemens, D. Dubrau, N. Tautz

Institute of Virology and Cell Biology, University of Lübeck, Lübeck, Germany

ABSTRACT

A peculiarity of the *Flaviviridae* is the critical function of nonstructural (NS) proteins for virus particle formation. For pestiviruses, like bovine viral diarrhea virus (BVDV), uncleaved NS2-3 represents an essential factor for virion morphogenesis, while NS3 is an essential component of the viral replicase. Accordingly, in natural pestivirus isolates, processing at the NS2-3 cleavage site is not complete, to allow for virion morphogenesis. Virion morphogenesis of the related hepatitis C virus (HCV) shows a major deviation from that of pestiviruses: while RNA replication also requires free NS3, virion formation does not depend on uncleaved NS2-NS3. Recently, we described a BVDV-1 chimera based on strain NCP7 encompassing the NS2-4B*-coding region of strain Osloss (E. Lattwein, O. Klemens, S. Schwindt, P. Becher, and N. Tautz, J Virol 86:427–437, 2012, doi:10.1128/JVI.06133-11). This chimera allowed for the production of infectious virus particles in the absence of uncleaved NS2-3. The Osloss sequence deviates in the NS2-4B* part from NCP7 in 48 amino acids and also has a ubiquitin insertion between NS2 and NS3. The present study demonstrates that in the NCP7 backbone, only two amino acid exchanges in NS2 (E1576V) and NS3 (V1721A) are sufficient and necessary to allow for efficient NS2-3-independent virion morphogenesis. The adaptation of a bicistronic virus encompassing an internal ribosomal entry site element between the NS2 and NS3 coding sequences to efficient virion morphogenesis led to the identification of additional amino acids in E2, NS2, and NS5B that are critically involved in this process. The surprisingly small requirements for approximating the packaging schemes of pestiviruses and HCV with respect to the NS2-3 region is in favor of a common mechanism in an ancestral virus.

IMPORTANCE

For positive-strand RNA viruses, the processing products of the viral polyprotein serve in RNA replication as well as virion morphogenesis. For bovine viral diarrhea virus, nonstructural protein NS2-3 is of critical importance to switch between these processes. While free NS3 is essential for RNA replication, uncleaved NS2-3, which accumulates over time in the infected cell, is required for virion morphogenesis. In contrast, the virion morphogenesis of the related hepatitis C virus is independent from uncleaved NS2-NS3. Here, we demonstrate that pestiviruses can adapt to virion morphogenesis in the absence of uncleaved NS2-3 by just two amino acid exchanges. While the mechanism behind this gain of function remains elusive, the fact that it can be achieved by such minor changes is in line with the assumption that an ancestral virus already used this mechanism but lost it in the course of adapting to a new host/infection strategy.

The family *Flaviviridae* comprises the genera *Flavivirus*, *Hepacivirus*, *Pestivirus*, and *Pegivirus* (1–3). Pestiviruses, like bovine viral diarrhea virus (BVDV) and classical swine fever virus (CSFV), are important pathogens causing significant economic damage in livestock industries (3). They are classified into 2 biotypes based on their ability to induce a cytopathic effect in cell culture: noncytopathic (ncp) or cytopathic (cp). Furthermore, they are close relatives of the human hepatitis C virus (HCV). The single-stranded, positive-sense RNA genome of pestiviruses has a length of approximately 12.3 kb and is comprised of a single open reading frame (ORF), which is flanked by 5′ and 3′ untranslated regions (UTR) (4). Translation results in the generation of a single polyprotein consisting of about 3,900 amino acids (aa). The sequential order of viral proteins in the polyprotein is NH_2-N^{pro} (N-terminal autoprotease), C (capsid protein, core), E^{rns} (envelope protein RNase secreted), E1, E2, p7, NS2-3 (NS2 and NS3), NS4A, NS4B, NS5A, and NS5B-COOH. The polyprotein is co- and posttranslationally processed by cellular and viral proteases. The N-terminal autoprotease N^{pro} generates its own C terminus and thereby also the N terminus of the capsid protein core. Further processing of structural proteins C, E^{rns}, E1, and E2, as well as of p7, is carried out by the endoplasmic reticulum (ER) resident proteases signal peptidase and signal peptide peptidase (4, 5). The downstream nonstructural proteins are processed by viral proteases NS2 and NS3-4A (4). NS2 has cysteine-autoprotease activity and catalyzes cleavage at the NS2-3 site (6). NS3 is a multifunctional protein and has serine protease, helicase, and NTPase activities (7–10). NS3 processes all downstream cleavage sites in concert with its cofactor, NS4A (11, 12). For pestiviruses, NS3, NS4A, NS4B, NS5A, and NS5B have been shown to assemble into the active viral RNA-replicase together with an unknown number

Received 25 June 2015 **Accepted** 4 September 2015

Accepted manuscript posted online 9 September 2015

Citation Klemens O, Dubrau D, Tautz N. 2015. Characterization of the determinants of NS2-3-independent virion morphogenesis of pestiviruses. J Virol 89:11668–11680. doi:10.1128/JVI.01646-15.

Editor: R. M. Sandri-Goldin

Address correspondence to N. Tautz, tautz@vuz.uni-luebeck.de.

O.K. and D.D. contributed equally to this work.

TABLE 1 BVDV-1 full-length clones used for the analysis of NS2-3-independent virion morphogenesis

Plasmid name	Feature(s)
pN7-388	Encompasses a full-length cDNA genome of BVDV-1 NCP7 (39, 40)
pN7/OsNS2-NS4B*	pNCP7-388 derivative coding for the NS2-4A region and 16 N-terminal aa of NS4B of BVDV-1 Osloss as well as selected mutations R1268Q in NS2 and A14324C in the 3′UTR; NS2 was inactivated by mutations C1512A and H1447A within the active site; previously published as pN7/OsNS2-4A(H/A,C/A)(R1268Q, 3′UTR) (34)
pN7/OsNS2-NS4B* GAA	Derivative of pN7/OsNS2-NS4B*; inactivated NS5B by mutations GDD to GAA; negative control for RNA replication
pN7/OsNS2-NS4B* (+N7/1643-1878)	Derivative of pN7/OsNS2-NS4B*; codes for aa 1643-1878 of strain NCP7
pN7/OsNS2-NS4B* (+N7/1878-2078)	Derivative of pN7/OsNS2-NS4B*; codes for aa 1878-2078 of strain NCP7
pN7/OsNS2-NS4B* (+N7/2078-2352)	Derivative of pN7/OsNS2-NS4B*; codes for aa 2078-2352 of strain NCP7
pN7/OsNS2-NS4B* (3/AV)	Derivative of pN7/OsNS2-NS4B*; codes for mutation A1721V in NS3
pN7/OsNS2-NS4B* (3/SN)	Derivative of pN7/OsNS2-NS4B*; codes for mutation S1791N in NS3
pN7/OsNS2-NS4B* (3/KR)	Derivative of pN7/OsNS2-NS4B*; codes for mutation K1811R in NS3
pN7/OsNS2 (3/VA)	Derivative of pN7/OsNS2-NS4B*; codes for aa 1643-2352 of strain NCP7 and mutation V1721A in NS3
pN7/OsUbi-NS4B* (2/RQ)	pNCP7-388 containing ubi-NS3-4A-4B* coding region of BVDV-1 strain Osloss; NS2 contains the mutation R1268Q, and protease active site was inactivated by mutation C1512A
pN7-2/EV-Ubi-3/VA	Derivative of pN7-388 encoding the ubiquitin monomer originating from strain Osloss between NS2 and NS3 genes (Ubi); NS2 protease was inactivated by the deletion of the active-site cysteine C1512; contains the mutations E1576V in NS2 (2/EV) and V1721A in NS3 (3/VA)
pN7-2/EX-Ubi-3/VA	Derivative of pN7-2/EV-Ubi-3/VA; aa E1576 is replaced by aa A, I, M, Y, Q, S, or R (represented by X)
pN7-2/EV-Ubi-3/VX	Derivative of pN7-2/EV-Ubi-3/VA; aa V1721 is replaced by aa I, M, Y, Q, S, E, or R (represented by X)
pN7-2/EV-IRES-3/VA	Bicistronic derivative of pN7-388; NS2 and NS3 genes are separated by an EMCV IRES sequence containing the mutations E1576V in NS2 (2/EV) and V1721A in NS3 (3/VA); NS2 protease was inactivated by deletion of the active-site cysteine C1512
pN7-2/EV-IRES-3/VA(E2/+K, 2/TA, 5B/EG)	Derivative of pN7-2/EV-IRES-3/VA, additionally containing mutations 906+K in E2 (E2/+K), T1405A in NS2 (2/TA), and E3324G in NS5B (5B/EG)

of host factors (4, 13). The structural proteins as well as N^{pro}, p7, and NS2 are not required for this process.

With regard to virion morphogenesis, the situation is more complex. It is known for the members of the *Flaviviridae* that besides the structural proteins, the nonstructural proteins also are critical for virion morphogenesis (14). For pestiviruses, almost all nonstructural proteins have been shown to be essential for the production of infectious viral particles (15–19). Pestiviral NS4B has not yet been characterized with regard to its role in virion morphogenesis but has been shown to be critical in HCV virion morphogenesis, suggesting a similar function in pestiviruses (20).

A special feature in the life cycle of noncytopathogenic (ncp) pestiviruses is the strictly regulated temporal processing of NS2-3 (21, 22). NS2 activation depends on the abundance of a cellular cofactor (6, 21). In cell culture, efficient NS2-3 cleavage is observed only during the early phase of infection due to a limiting amount of the activating cofactor Jiv (J-domain protein interacting with viral protein), leading to the accumulation of uncleaved NS2-3 at later time points (6). The downregulation of NS2-3 cleavage is required to retain the ncp phenotype that is a prerequisite for the establishment of persistent infections upon intrauterine infections. These infections may lead to persistently infected calves, which represent a reservoir for the virus (3, 23).

In persistently infected animals, the emergence of a cp virus, which is often caused by RNA recombination, induces the onset of lethal mucosal disease (MD) (23–26). The induction of the cp phenotype correlates with an uncontrolled/unregulated production of free NS3, leading to an upregulation of RNA replication

TABLE 2 Subgenomic reporter plasmids used for the analysis of RNA replication efficiency

Plasmid name	Feature(s)
pBici RLuc NS2-3′	Bicistronic BVDV reporter gene construct; the 5′ ORF encodes N^{pro} followed by *Renilla* luciferase; the 3′ ORF encodes the CP7 BVDV proteins NS2-5B (18)
pBici RLuc NS2-3′ GAA	Derivative of pBici RLuc NS2-3′; inactivation of NS5B by mutation of GDD to GAA; negative control for RNA replication
pBici RLuc NS2-3′ (3/VA)	Derivative of pBici RLuc NS2-3′; contains mutation V1721A in NS3
pBici RLuc NS2-3′ (5B/EG)	Derivative of pBici RLuc NS2-3′; contains mutation E3325G in NS5B
pBici RLuc NS2-3′ (3/VA,5B/EG)	Derivative of pBici RLuc NS2-3′; contains mutation V1721A in NS3 and E3325G in NS5B
pBici RLuc NS3-3′	Bicistronic BVDV reporter gene construct; the 5′ ORF encodes N^{pro} followed by *Renilla* luciferase; the 3′ ORF encodes the viral replicase NS3-5B (18)
pBici RLuc NS3-3′ GAA	Derivative of pBici RLuc NS3-3′; inactivated NS5B by mutation of GDD to GAA; negative control for RNA replication
pBici RLuc NS3-3′ (V1721X)	Derivative of pBici RLuc NS3-3′; aa V1721 is replaced by aa A, I, M, Y, Q, S, E, or R (represented by X)

and the induction of apoptosis (6, 27–31). The increased production of free NS3 in cp viruses often is based on genomic alterations in the NS2-3 coding region (23, 25). In this context, different insertions of cellular RNA sequences have been identified in NS2-3, each resulting in the enhanced processing of NS2-3 (23). Insertions of cellular ubiquitin-coding sequences lead to highly efficient processing by cellular ubiquitin C-terminal hydrolases (UCHs), thereby generating the authentic N terminus of NS3. Earlier studies demonstrated that the artificial insertion of either a ubiquitin-coding sequence or an IRES (internal ribosomal entry site) element between the NS2 and NS3 genes abolishes infectious virus particle formation (15, 19). According to these studies, uncleaved NS2-3 was regarded as an essential factor for pestiviral virion morphogenesis.

In contrast, in the HCV cell culture system, uncleaved NS2-NS3 is not essential for infectious particle production. In cell culture, the processing of HCV NS2-NS3 is very efficient, and the insertion of an IRES between the NS2 and NS3 genes has no major impact on virion production (32, 33). This remarkable difference between these closely related genera was challenged recently by a study of Lattwein and coworkers which demonstrated the possibility of NS2-3-independent virion morphogenesis for a pestivirus (34). This chimeric virus was based on ncp BVDV-1 strain NCP7 and contained the NS2-4B* region of cp BVDV-1 strain Osloss (4B* indicates the 16 N-terminal Osloss-specific amino acids). The Osloss sequence deviates in the NS2-4B* part from the one of NCP7 in 48 amino acids, as well as in an Osloss-specific ubiquitin insertion located upstream of NS3. Efficient virion morphogenesis of the chimeric virus required an adaptive mutation in NS2 (R1268Q) and an authentic stem-loop 1 (SL1) in the 3′UTR (34). Titer-enhancing mutations were selected in E^{rns}, E2, and p7. However, for this virus it was not determined which of the mutations are critical for NS2-3-independent virion morphogenesis or represent adaptations to compensate for the chimeric nature of the virus.

The present study addressed this question and succeeded in identifying the minimal set of amino acid exchanges necessary and sufficient for NS2-3-independent virion morphogenesis in the context of BVDV strain NCP7: two amino acid exchanges, one in NS2 and one in NS3. Studies using an NS2-IRES-NS3 bicistronic virus genome identified additional regions in E2, NS2, and NS5B involved in the process of virion morphogenesis.

In conclusion, this study demonstrates that pestiviruses can adapt by minor changes to a virion morphogenesis scheme which does not require uncleaved NS2-3, a situation analogous to the HCV system. Moreover, the obtained virus mutants represent highly valuable tools for future analyses of the underlying mechanism and the molecular dissection of protein complexes required for pestiviral particle formation.

MATERIALS AND METHODS

Cells and viruses. Madin Darby bovine kidney (MDBK) cells were cultivated in minimal essential medium (MEM; Invitrogen, Karlsruhe, Germany) containing 10% horse serum and 1% penicillin-streptomycin (PAA, Pasching, Austria). Huh7-T7 cells were kept in DMEM containing 10% fetal bovine serum, 1% penicillin-streptomycin, and 125 μg/ml G418 (PAA, Pasching, Austria). All cells were grown at 37°C and 5% CO_2. BVDV-1 strains NCP7 and Osloss were described previously (35, 36). Vaccinia virus modified virus Ankara (MVA)-T7pol (37) was generously provided by G. Sutter (LMU, Munich, Germany).

TABLE 3 Subgenomic expression plasmids used for the analysis of polyprotein processing

Plasmid name	Feature(s)
pT7-DI-388	Subgenomic replicon based on BVDV pDI9 and strain CP7, encoding N^{pro}-NS3-5B viral proteins (13); in contrast to pDI9, the RNA transcription is under the control of a T7-promoter
pT7-DI-388 (S1752A)	Derivative of pT7-DI-388; inactivation of NS3 protease by mutation of the active-site serine S1752 to alanine
pT7-DI-388 (V1721X)	Derivative of pT7-DI-388; aa V1721 is replaced by aa A, E, I, Q, S, Y, R, or M (represented by X)

Antibodies. For the detection of BVDV NS3/NS2-3, anti-NS3/NS2-3 mouse monoclonal antibody 8.12.7 (38) was used. For the detection of BVDV nonstructural protein antibodies, GH4A1 (4B7) (NS4A), GL4B1 (NS4B), GLBVD5A1 (11C) (NS5A), and GLBVD5B1 (9A) (NS5B), kindly provided by T. Rümenapf and B. Lamp (University of Veterinary Medicine, Vienna, Austria), were used (18). Species-specific fluorescent dye-conjugated secondary antibodies were obtained from Dianova (Hamburg, Germany). For Western blot analysis, goat anti-mouse IgG antibody coupled to horseradish peroxidase was used as the secondary antibody (Dianova, Hamburg, Germany).

Construction of recombinant BVDV plasmids. Complete overviews of the constructs used in this study are shown in Tables 1 to 3. Plasmids were generated by standard cloning techniques. Mutations were inserted by PCR or the QuikChange mutagenesis method (Stratagene, Heidelberg, Germany). All constructs were verified by restriction enzyme digestion and sequencing. Table 1 summarizes all full-length constructs used in this study. Detailed information of cloning strategies and exact sequences can be obtained upon request. All constructs used in this study are based on either pN7/OsNS2#(RQ)-4B*(3′UTR) (34) or pNCP7-388 backbones (39, 40).

DNA transfection and eukaryotic protein expression. Transfections were carried out in 6-well cell culture plates (TPP, Trasadingen, Switzerland). Approximately 3×10^6 Huh7-T7 cells, which express T7 RNA polymerase (41), were infected additionally with modified vaccinia virus Ankara-T7pol (MVA-T7pol) for 1 h to increase T7 RNA polymerase levels. Following infection, cells were transfected with 4 μg of plasmid DNA by using 10 μl Superfect transfection reagent (Qiagen, Hilden, Germany). Protein expression was carried out overnight, and cells were further processed for SDS-PAGE.

***In vitro* transcription and RNA electroporation.** Two micrograms of plasmid DNA were linearized with SmaI and used as the template for transcription with a MAXIscript SP6 transcription kit (Ambion, Huntingdon, United Kingdom). The amount of RNA was determined by using a Quant-iT RNA assay kit and Qubit fluorometer (Invitrogen, Karlsruhe, Germany). RNA quality was verified by agarose gel electrophoresis. All RNAs of one experiment were generated and analyzed in parallel. One microgram of RNA was used for electroporation of 3×10^6 MDBK cells. The electroporation of RNAs in MDBK cells was carried out as described in reference 42 by using a Bio-Rad Xcell gene pulser.

SDS-PAGE and Western blotting. Cell lysates were analyzed on SDS-polyacrylamide-tricine gels (8 or 10% polyacrylamide) (43). Following electrophoresis, proteins were transferred onto a nitrocellulose membrane. Membranes were blocked with 5% (wt/vol) skim milk powder (Roth, Karlsruhe, Germany) in phosphate-buffered saline (PBS)-Tween 20 (0.05%, vol/vol). Viral proteins were detected with the indicated monoclonal antibodies and visualized with the corresponding peroxidase-coupled species-specific secondary antibodies and Western Lightning plus enhanced chemiluminescence reagent (PerkinElmer, Boston, MA).

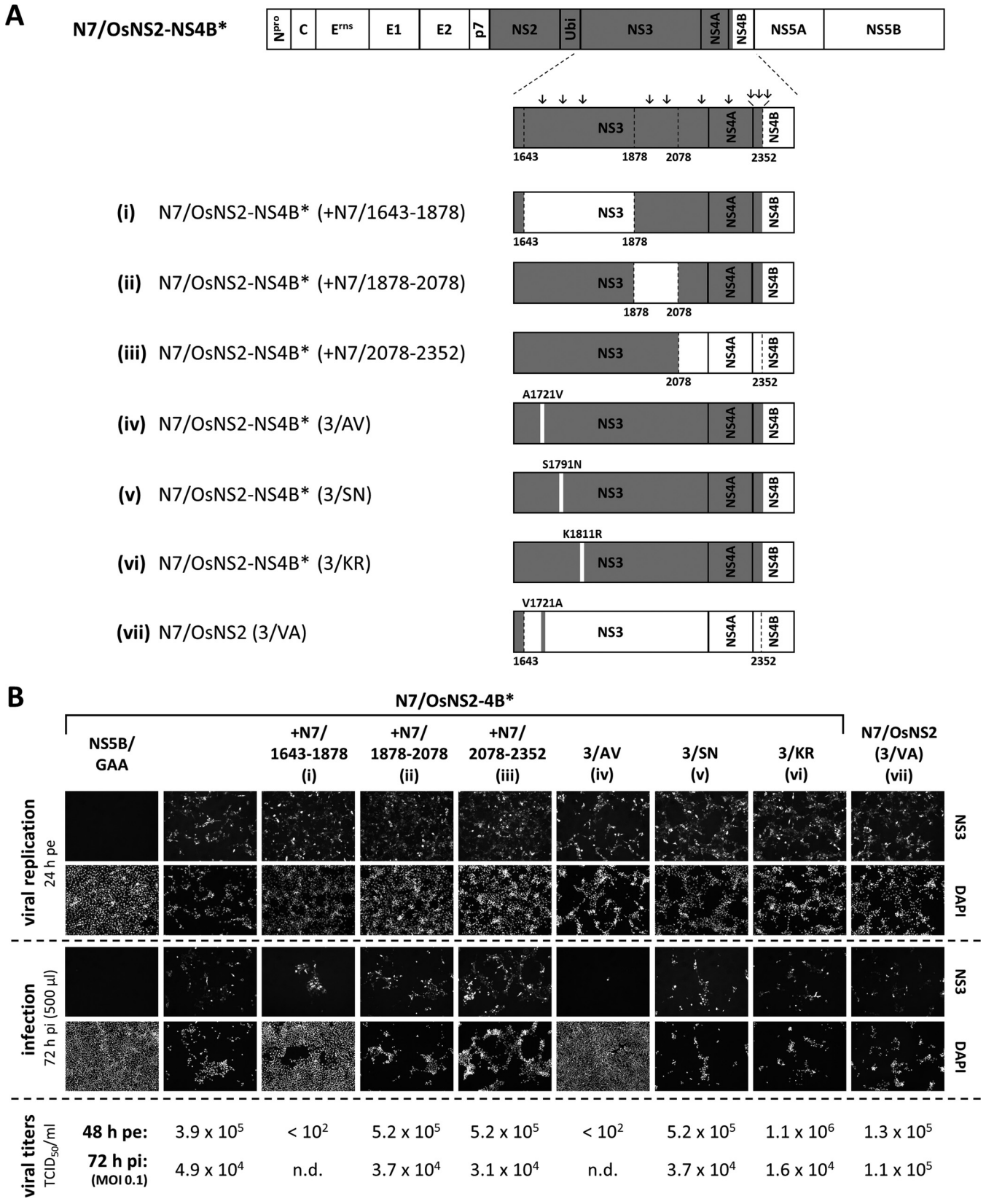

FIG 1 Amino acid 1721 within NS3 is critical for NS2-3-independent virion morphogenesis. (A) Scheme of the virus chimeras. All chimeras are based on N7/OsNS2-NS4B* (34). Rows i to vii depict the NS3-4A-4B region of the corresponding chimeric virus derivatives. NS3 amino acid sequences N terminal of position 1643 are identical in Osloss and NCP7 but show differences on the nucleic acid level. Dotted lines mark borders of exchanged sequence regions, and the corresponding amino acid positions are indicated. Gray, Osloss sequence; white, NCP7 sequence; (↓), difference in the amino acid sequence between strains

Luciferase assay. To quantify RNA replication efficiencies, bicistronic reporter constructs encoding N^{pro}-*Renilla* luciferase in the 5′ ORF and the viral replicase NS3-5B or NS2-5B in the 3′ ORF were used (18). To analyze luciferase activity, *Renilla* glow juice (PJK, Kleinblittersdorf, Germany) was applied as described in the manufacturer's instructions. Approximately 3×10^6 cells were lysed in 40 μl lysis juice. Twenty microliters of cell lysates were mixed with 100 μl of *Renilla* glow juice, and relative light units (RLUs) were measured with a Junior LB 9509 portable tube luminometer (Berthold Technologies, Bad Wildbad, Germany).

Nucleotide sequencing. Sequence data obtained from Qiagen genomics services (Hilden, Germany) or LGC genomics (Berlin, Germany) were further analyzed by using Vector NTi Advance 11.5.1 (Invitrogen, Karlsruhe, Germany).

RNA isolation, reverse transcription-PCR (RT-PCR), and direct sequencing of viral genomes. RNA derived from BVDV-infected cells was isolated by using an RNeasy RNA isolation kit (Qiagen, Hilden, Germany). Alternatively, RNA was isolated from viral particles in cell culture supernatants via a QIAamp viral RNA kit (Qiagen, Hilden, Germany). cDNA fragments were generated by using Superscript II reverse transcriptase (Invitrogen, Karlsruhe, Germany) and the Expand long template PCR system (Roche, Mannheim, Germany). Primer sequences can be obtained upon request. The amplicons were purified by agarose gel electrophoresis, followed by gel elution with a QIAquick gel extraction kit (Qiagen, Hilden, Germany), and were directly sequenced with appropriate sequencing primers.

RESULTS

One amino acid in BVDV NS3 is critical for virion morphogenesis in the absence of uncleaved NS2-3. It has been shown before that the NS2-4B* coding region of BVDV Osloss is sufficient to allow for virion morphogenesis in the absence of uncleaved NS2-3 in the context of a chimeric virus that carries either a ubiquitin gene or an encephalomyocarditis virus (EMCV)-IRES between the NS2 and NS3 coding regions (34). This virus contains the Osloss genes NS2, NS3, and NS4A and the first 48 bp of NS4B (NS4B*) in a NCP7-388 backbone. In addition, the mutation R1268Q in NS2 and the wt SL1 sequence in the 3′UTR were present, which have been shown to be critical in the context of this NCP7/Osloss chimera (34). In the present study, this chimera, termed N7/OsNS2-NS4B*, was used as a starting point (Fig. 1A).

Six of the Osloss-specific amino acid differences in the chimera are located in NS3, one in NS4A, and three in the NS4B* fragment. To identify critical amino acid positions in NS3-NS4B* required for NS2-3-independent virion morphogenesis, a stepwise exchange of the Osloss NS3-NS4B* genome fragments by the corresponding NCP7 cDNAs was performed (Fig. 1A, i to iii). In a first step, the virus chimeras were tested for their RNA replication capability. In the pestivirus system, the detection of NS3 at 24 h postelectroporation (pe) by an immunofluorescence (IF) assay is known to be indicative of active RNA replication (13). The results clearly indicate that all chimeric derivatives replicate their genome (Fig. 1B, top rows). In contrast, electroporation of a replication-defective control genome (N7/OsNS2-4B* NS5B/GAA) did not lead to detectable amounts of NS3. Thus, the fragment substitutions tested cause no obvious defects in viral RNA replication. However, the analysis of the virion morphogenesis capabilities of these chimeras revealed that only in chimera N7/OsNS2-NS4B* (+N7/1643-1878), with an alteration of the N-terminal part of NS3, was virion morphogenesis severely reduced, resulting in small amounts of NS3-positive cells, the lack of a cytopathic effect (Fig. 1B, middle rows, compare NS3 and 4′,6-diamidino-2-phenylindole [DAPI] staining for i to iii), and low virus titers (Fig. 1B, bottom rows). The other two tested variants (Fig. 1A, ii and iii) did not lead to detectable differences in virion production compared to that of N7/OsNS2-NS4B* (Fig. 1B, bottom rows). These findings demonstrate the importance of the N-terminal region of Osloss NS3 for virion morphogenesis in the absence of uncleaved NS2-3. In this region, the Osloss and NCP7 sequences differ at three amino acid positions: 1721 (Osloss-A, NCP7-V), 1791 (Osloss-S, NCP7-N), and 1811 (Osloss-K, NCP7-R).

In the next step, each of these Osloss-specific amino acids was individually changed to the amino acid present in the NCP7 strain, resulting in the virus mutants N7/OsNS2-NS4B*(3/AV), N7/OsNS2-NS4B*(3/SN), and N7/OsNS2-NS4B*(3/KR) (Fig. 1A, iv to vi). As expected, all of these mutants showed RNA replication at 24 h pe (Fig. 1B, top rows). Furthermore, mutations SN and KR had no effect on viral titers compared to N7/OsNS2-NS4B* (Fig. 1B, bottom rows). In contrast, mutation 3/AV abolishes virion production almost completely (Fig. 1B, middle and bottom rows), revealing the importance of amino acid position 1721 in NS3 for NS2-3-independent virion morphogenesis.

To verify the critical role of position 1721, a reverse amino acid change, 3/VA, was inserted in a chimeric virus that contains amino acids 1643 to 2352 of NCP7, generating N7/OsNS2 (3/VA) (Fig. 1A, vii). Efficient virion production by this chimera finally demonstrates that mutation V1721A in NS3 is the only mutation outside NS2 required for rescuing virion morphogenesis in the absence of uncleaved NS2-3 (Fig. 1B, bottom rows).

Adaptation of a chimeric BVDV to efficient NS2-3-independent virion morphogenesis in cell culture depends on mutation E1576V in NS2. Due to numerous amino acid differences in the NS2 region between strains NCP7 and Osloss, a functional analysis by individual amino acid exchanges was not feasible. Therefore, a cell culture-based adaptation approach was applied. Accordingly, chimera N7/OsUbi-NS4B*(2/RQ), which is based on N7/OsNS2-NS4B* but contains only the Ubi-NS3-4A-4B* region of BVDV Osloss and, as a result, the NS3 determinant for NS2-3-independent virion morphogenesis in a NCP7 backbone, was generated (Fig. 2). The NS2 protease was inactivated by an active-site mutation (see Materials and Methods and Table 1), rendering the ubiquitin insertion essential for the production of free NS3 and ensuring the retention of the ubiquitin gene during passaging. The experiment was carried out in 12 replicates to identify adaptations of the NS2 sequence which promote virion morphogenesis.

NS3-specific IF at 24 h pe and 48 h pe confirmed RNA replica-

Osloss and NCP7; NS4B*, 16 N-terminal amino acids of NS4B; (3/AV), amino acid exchange A1721V in Osloss NS3; (3/SN), amino acid exchange S1791N in Osloss NS3; (3/KR), amino acid exchange K1811R in Osloss NS3; (3/VA), amino acid exchange V1721A in NCP7 NS3. (B) Detection of viral replication and virion morphogenesis of different NCP7/Osloss chimeras. MDBK cells were electroporated with 1 μg of *in vitro*-transcribed RNA. (Top) Detection of viral replication was carried out by NS3-specific IF 24 h pe. Supernatants were harvested 48 h pe. (Middle) Naive MDBK cells were inoculated with 500 μl of cell culture supernatant. Infected cells were visualized by detection of NS3 via IF 72 h pi. (Bottom) Viral titers 48 h pe and 72 h pi after infection at an MOI of 0.1. Data are representative of three independent experiments. Chimeric virus derivatives used in the experiments are indicated at the top, and (i-vii) correspond to the respective construct described for panel A. NS5B/GAA, N7/OsNS2-4B* replication-deficient negative control; n.d., not determined.

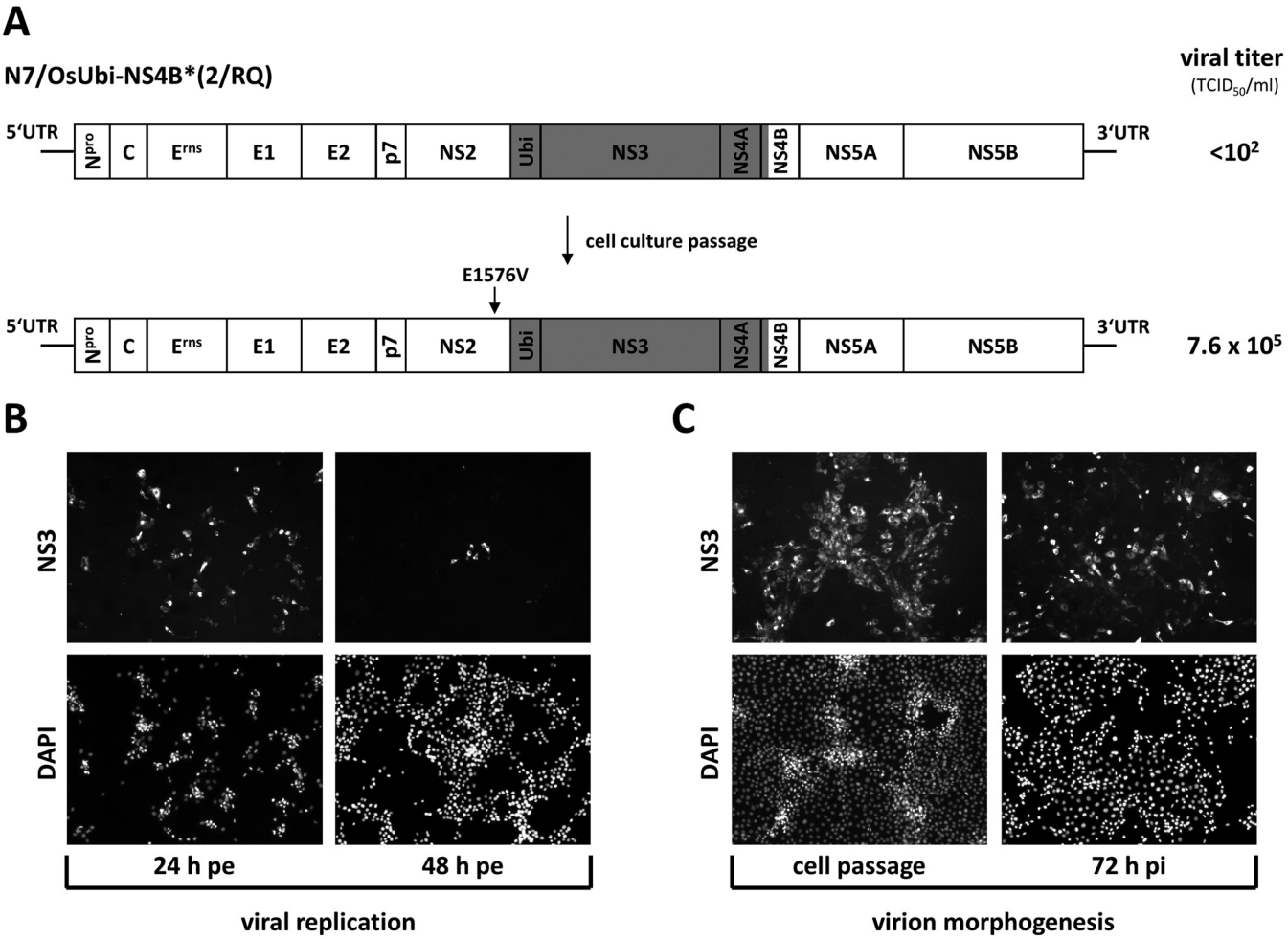

FIG 2 Identification of E1576V in NS2 as a critical determinant for efficient NS2-3-independent virion morphogenesis. (A) Schematic drawing of N7/OsUbi-NS4B*(2/RQ). Cell culture passages of N7/OsUbi-NS4B*(2/RQ) identified the mutation E1576V in NS2 that is critical for NS2-3-independent virion morphogenesis, resulting in increased viral titers of 7.6×10^5 $TCID_{50}$/ml. Osloss sequences are shown in gray. 2/RQ, cell culture-adapted mutation in NS2 at position 1268 (34). Ubi, ubiquitin insertion derived from BVDV strain Osloss. Viral titers were determined in $TCID_{50}$/ml. (B) MDBK cells were electroporated with 1 μg of RNA of the chimeric BVDV derivative N7/OsUbi-NS4B*(2/RQ). Cell cultures grown for 24 h and 48 h pe were analyzed by NS3-specific IF. (C) Electroporated cells depicted in panel B were passaged until an increased cytopathic effect was observed (cell passage) and cell culture supernatants were collected. Naive MDBK cells were inoculated with 500 μl of the collected supernatants and analyzed by NS3-specific IF at 72 h pi. Viral RNAs were isolated and the NS2-3-4A-4B* region was sequenced. Analyses identified the mutation E1576V in NS2.

tion (Fig. 2B), but as expected, N7/OsUbi-NS4B*(2/RQ) produced only very low levels of infectious viruses at 48 h pe (below 10^2 50% tissue culture infectious doses [$TCID_{50}$]/ml) (Fig. 2A, top). The electroporated cells were passaged until an increased cytopathic effect and higher percentage of NS3-positive cells were detected (Fig. 2C, left), while the viral titers of those cultures increased (7.6×10^5 $TCID_{50}$/ml) (Fig. 2A, bottom). Subsequently, supernatants were used to infect naive MDBK cells (Fig. 2C, right), and the NS2-3-4A-4B* region of the 12 selected virus derivatives was analyzed by RT-PCR and direct sequencing. For 11 of 12 samples, nucleotide sequences could be determined. In all sequences one NS2 mutation, leading to exchange E1576V (2/EV), was identified, while no changes were detected in the NS3 sequence. In two of the selected viruses, one additional NS2 mutation besides E1576V was identified, leading to exchange Y1381H or Y1524C. These mutations were not pursued further, because they were only found in single samples. Since the passaged viruses were not cloned by plaque purification, one cannot exclude the presence of additional mutations encoded by a small fraction of viruses in the selected virus population, which were not detected due to the chosen experimental setup. Interestingly, valine found in all passaged viruses at position 1576 is the Osloss-specific amino acid present in the NS2 protein at this position (see Fig. 7). This finding suggested that valine 1576 exerts a critical role during virion morphogenesis in the absence of uncleaved NS2-3.

Two amino acid exchanges are sufficient to allow efficient virion morphogenesis in a nonchimeric monocistronic virus but not in a bicistronic virus. The previously described results were obtained using chimeric BVDV-1 constructs. Based on those findings, the minimal set of mutations that is sufficient for NS2-3-independent virion morphogenesis in a nonchimeric virus should be determined. Accordingly, an NCP7-388 virus containing a ubiquitin insertion between NS2 and NS3, as well as the previously identified mutations in NS2 (2/EV) and NS3 (3/VA),

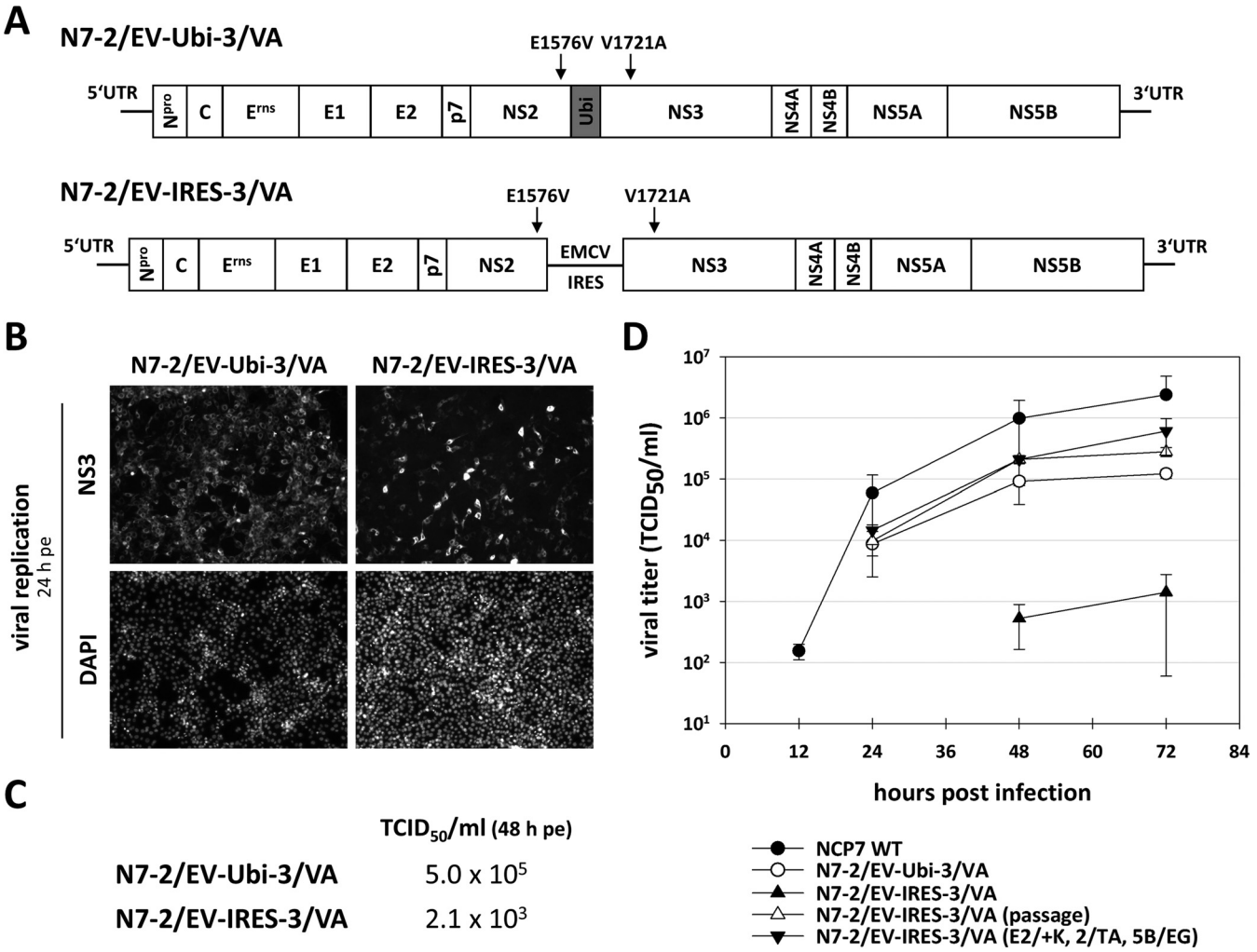

FIG 3 Virion morphogenesis in the absence of uncleaved NS2-3 in nonchimeric viruses. (A) Schematic drawing of the genome organizations of N7-2/EV-Ubi-3/VA and N7-2/EV-IRES-3/VA. Ubi, ubiquitin insertion. The mutations within NS2 (E1576A) and NS3 (V1721A) are indicated. (B) One microgram of the RNA genomes depicted in panel A were electroporated into MDBK cells. Viral replication was visualized by NS3-specific IF at 24 h pe. (C) At 48 h pe, viral supernatants were harvested and analyzed for the presence of infectious viruses. Viral titers were determined as $TCID_{50}$/ml. (D) Growth curve analysis. MDBK cells were infected with the indicated viruses at an MOI of 0.1, and viral growth was analyzed for 72 h. At the indicated time points, supernatants were collected and viral titers were determined (in $TCID_{50}$/ml). Analyzed viruses include N7-2/EV-Ubi-3/VA, N7-2/EV-IRES-3/VA, N7-2/EV-IRES-3/VA (passage), and the N7-2/EV-IRES-3/VA derivative, which encompasses all three titer-enhancing mutations in E2, NS2, and NS5B (E2/+K, 2/TA, and 5B/EG). NCP7 WT, wild type. Mean values from three independent experiments and standard deviations are depicted.

was generated (N7-2/EV-Ubi-3/VA) (Fig. 3A, top). The NS2 protease of this virus was inactivated by the deletion of the active-site cysteine (see Materials and Methods and Table 1). As expected, N7-2/EV-Ubi-3/VA was able to replicate its RNA (Fig. 3B, left) and to produce titers of 5.0×10^5 $TCID_{50}$/ml at 48 h pe (Fig. 3C). Also upon infection, infectious particle production was highly efficient and reached titers of 1.5×10^5 $TCID_{50}$/ml (multiplicity of infection [MOI] of 0.1 at 72 h pi) as determined by growth kinetics analysis (Fig. 3D).

In parallel, a bicistronic NCP7 derivative, N7-2-IRES-3, containing the encephalomyocarditis virus IRES between the NS2- and NS3-coding regions, was generated. The NS2-protease of this virus was inactivated by the deletion of the active-site cysteine (see Materials and Methods and Table 1). This construct allows a more stringent separation of NS2 and NS3, since the two proteins are translated from individual ORFs. From this bicistronic construct, virus derivative N7-2/EV-IRES-3/VA was generated (Fig. 3A, bottom) to analyze its ability to produce infectious virus particles. As expected, this virus displayed efficient RNA replication (Fig. 3B, right). However, virus yields were very low, with titers of about 2.1×10^3 $TCID_{50}$/ml at 48 h pe (Fig. 3C). This finding was confirmed by a growth curve analysis, which revealed titers were 100-fold lower for the bicistronic N7-2/EV-IRES-3/VA than for the monocistronic N7-2/EV-Ubi-3/VA virus at 72 h pi (Fig. 3D).

Serial cell culture passages and biological cloning of the bicistronic virus improves virion morphogenesis efficiency and reveals 3 additional mutations supporting virion morphogenesis. In order to improve virion morphogenesis efficiency of N7-2/EV-IRES-3/VA, serial cell culture passages of virus-containing cell culture supernatants were performed. After 9 passages of cell culture supernatants, an increased cytopathic effect was detected that correlated with an increased number of NS3-positive cells. A virus

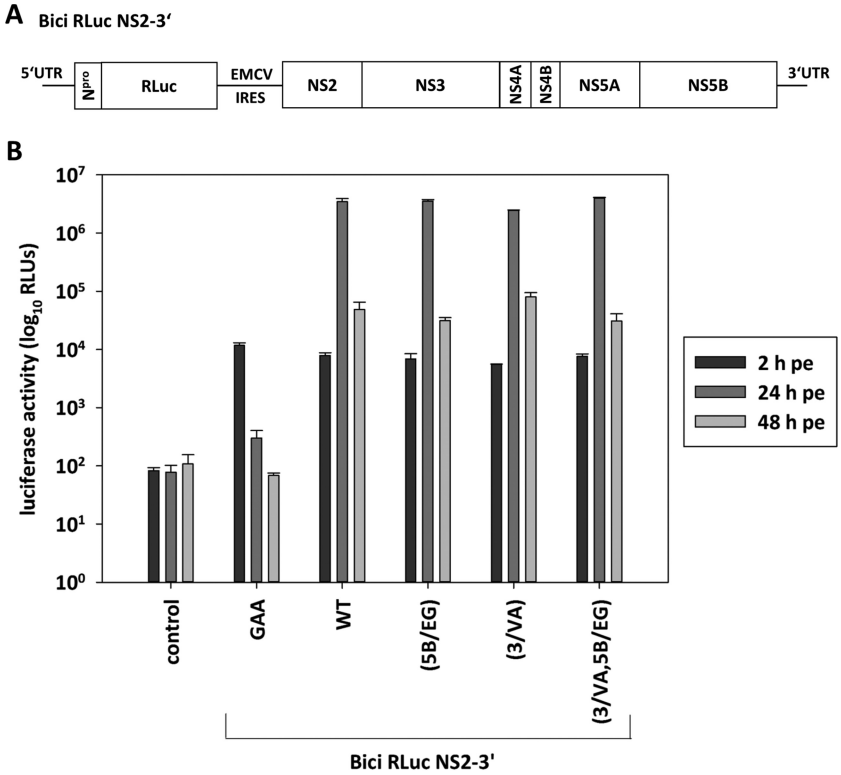

FIG 4 Selected mutations in NS3 (3/VA) and NS5B (5B/EG) do not show an impact on RNA replication. (A) Scheme of the bicistronic reporter replicon Bici RLuc NS2-3′. (B) MDBK cells were electroporated with 1 μg of the corresponding RNAs, and luciferase activity was determined at 2, 24, and 48 h pe. Measurements were carried out in triplicates, and experiments were repeated at least 3 times. Data from one representative experiment is shown. Error bars represent standard deviations. Control, no RNA electroporated; GAA, NS5B mutation, replication deficient; WT, wild type; RLUs, relative light units; RLuc, *Renilla* luciferase.

clone obtained after three consecutive rounds of plaque purification reached titers of 2.5×10^5 $TCID_{50}$/ml (72 h pi after infection at an MOI of 0.1) (Fig. 3D, N7-2/EV-IRES-3/VA [passage]). The genome sequence of this virus revealed three additional mutations: one in E2, which is an additional lysine residue following position 906 (E2/+K), one in NS2 (T1405A, 2/TA), and one in NS5B (E3324G, 5B/EG). These mutations were introduced into the N7-2/EV-IRES-3/VA virus genome, resulting in clone N7-2/EV-IRES-3/VA (E2/+K, 2/TA, and 5B/EG). The latter virus was able to produce titers comparable to that of the passaged virus N7-2/EV-IRES-3/VA (passage), as shown by growth curve analysis (Fig. 3D). Further analyses revealed that only a virus carrying a combination of all three additional mutations was able to reach high titers, while the induction of single or double mutations had only minor effects on virion morphogenesis (data not shown).

Accordingly, we identified two mutations in replicase proteins which could influence viral RNA replication capacity: E3324G in the viral RNA-dependent RNA polymerase NS5B and V1721A in the multifunctional protein NS3. IF staining of NS3, performed to analyze viral replication of full-length clones (Fig. 1B), allows no reliable quantitative assessment of viral RNA replication. To obtain such data, a luciferase reporter replicon assay was applied. To this end, E3324G (NS5B) and V1721A (NS3) were introduced alone and in combination into the bicistronic replicon Bici RLuc NS2-3′ (18). Interestingly, no effect on RNA replication efficiency was observed for the individual mutations or their combination (Fig. 4).

Identity of the amino acids 1576 (NS2, 2/EV) and 1721 (NS3, 3/VA) is critical for virion morphogenesis in the absence of uncleaved NS2-3. To determine the amino acid requirements at positions 1576 and 1721 for virion morphogenesis, a comprehensive mutagenesis study was conducted in the context of genome N7-2/EV-Ubi-3/VA. The individual viral genomes were electroporated in MDBK cells and analyzed for RNA replication and virion morphogenesis.

As expected, an IF analysis at 24 h pe revealed for all permutations of NS2 E1576 RNA replication competence, since NS2 is not required for RNA replication (Table 4). At 48 h pe, cell culture supernatants were harvested and viral titers were determined (Table 4). This analysis revealed that N7-2-Ubi-3/VA derivatives carrying NS2 mutations 2/EA, 2/EQ, 2/ES, and 2/ER did not produce infectious viral particles, while derivatives 2/EI, 2/EM, and 2/EY were able to generate infectious progeny. Virus titer determination showed that only mutant N7-2/EY-Ubi-3/VA reached a titer comparable to that of N7-2/EV-Ubi-3/VA (Table 4).

NS3 is a multifunctional protein. With its protease, helicase, and NTPase activities, NS3 is an essential component of the viral RNA replication complex. Accordingly, the effects of the permutations at position 1721 located in the NS3 protease domain on RNA replication were determined. For this purpose, representatives of all amino acid classes were introduced into the bicistronic reporter replicon Bici RLuc NS3-3′ at position 1721 in NS3 (Table 2) and analyzed for their ability to support RNA replication (Fig. 5). The bicistronic replicon derivatives

TABLE 4 Functional analysis of amino acid permutations at position 1576 in NS2[a]

aa E1576 (NS2) change	aa characteristic(s)	RNA replication	Viral titer 48 h pe[b] ($TCID_{50}$/ml)
Valine	Nonpolar/hydrophobic	+	5.0×10^5
Alanine	Nonpolar/hydrophobic	+	—
Isoleucine	Nonpolar/hydrophobic	+	4.9×10^4
Methionine	Nonpolar/hydrophobic	+	1.5×10^4
Tyrosine	Polar/neutral	+	2.3×10^5
Glutamine	Polar/neutral	+	—
Serine	Polar/neutral	+	—
Arginine	Basic	+	—

[a] Amino acids indicated were used to alter the glutamic acid at position 1576 in the context of N7-2/EV-Ubi-3/VA. Data shown are from one representative experiment out of 3 independent experiments.
[b] A dash indicates no infectious viruses were detected at 48 h pe.

with exchanges NS3 1721 VA, VI, VM, VY, and VQ replicated to levels comparable to those of the wild type (wt) (Fig. 5B). In contrast, the analysis also revealed that exchanges VS, VE, and VR do affect viral RNA replication to different degrees (Fig. 5B). While amino acid alterations to either glutamic acid or arginine were RNA replication deficient, similar to the RNA replication-deficient NS5B mutant (GAA), the serine mutant partially recovered to detectable RNA replication levels at 48 h pe, suggesting a delay in this process (Fig. 5B).

For the three NS3 mutants that were found to interfere with RNA replication, it seemed possible that their defects originate from alterations of their NS3-4A protease function. Accordingly, the viral polyprotein fragment N^{pro}-NS3-5B was expressed in an RNA replication-independent fashion using plasmid pT7-DI-388 and the MVA-T7pol system (Fig. 6A and Table 3). All tested pT7-DI-388 derivatives with V1721 mutations showed the authentic viral proteins (Fig. 6B). However, the experiments revealed that exchanges VE, VQ, VS, and VR at position 1721 cause an accumulation of protein precursors. The anti-NS3 antibody detected a protein of the calculated size of the NS3-4A-4B and NS3-5B precursors. Antibodies against NS4A detected protein precursors of the size of NS4A-4B and NS3-5B, respectively (Fig. 6B). In conclusion, this experiment revealed alterations in polyprotein processing for three derivatives which also exhibited defects in RNA replication (compare Fig. 5B and 6B).

In the next step, all mutants which showed RNA replication (Fig. 5B and Table 5) were analyzed for virion morphogenesis in an N7-2/EV-Ubi-3 background. Surprisingly, besides the derivative N7-2/EV-Ubi-3/VA, only the mutant N7-2/EV-Ubi-3/VS was able to generate infectious progeny (Table 5).

Taken together, the results obtained demonstrated that position 1721 is highly critical for polyprotein processing, RNA replication, and NS2-3-independent virion morphogenesis.

DISCUSSION

An interesting feature common to all members of the *Flaviviridae* family is the critical function of NS proteins not only during RNA replication but also for the production of infectious virus particles, as reviewed by Murray et al. (14). In this family, pestiviruses and the hepatitis C virus share a high degree of similarity but also show sufficient differences to make comparative studies on basic mechanisms of RNA replication and virion morphogenesis highly attractive. A striking difference between the strategies of these vi-

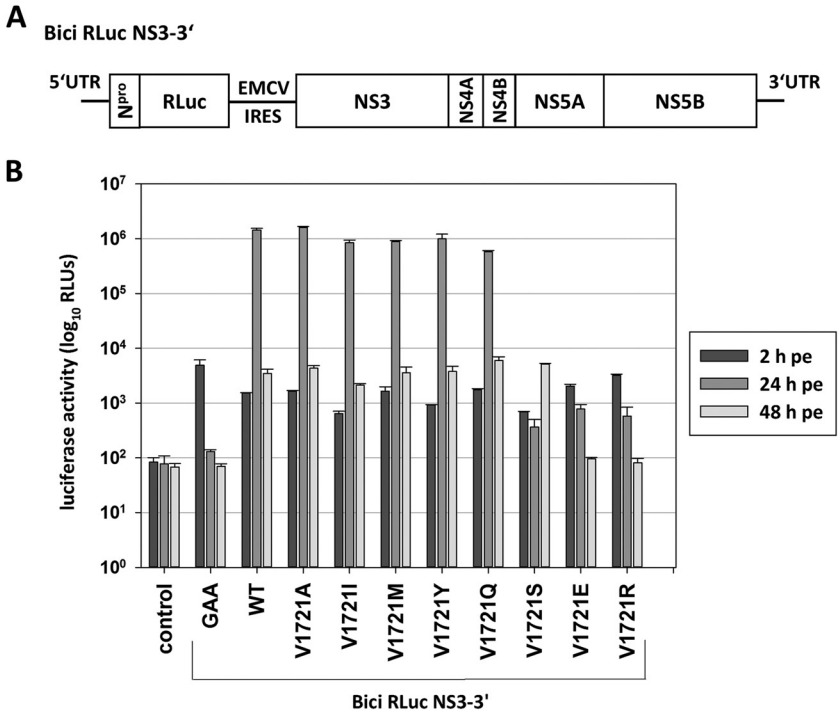

FIG 5 Character of amino acid V1721 in NS3 influences RNA replication. (A) Scheme of the bicistronic reporter replicon Bici RLuc NS3-3′. (B) MDBK cells were electroporated with 1 μg of the corresponding RNAs, and luciferase activity was determined at 2, 24, and 48 h pe. Measurements were carried out in triplicates, and experiments were repeated 3 times. Data from one representative experiment are shown. Error bars represent standard deviations. Control, no RNA electroporated; GAA, NS5B mutation, replication deficient; WT, wild type (V1721); RLUs, relative light units; RLuc, *Renilla* luciferase.

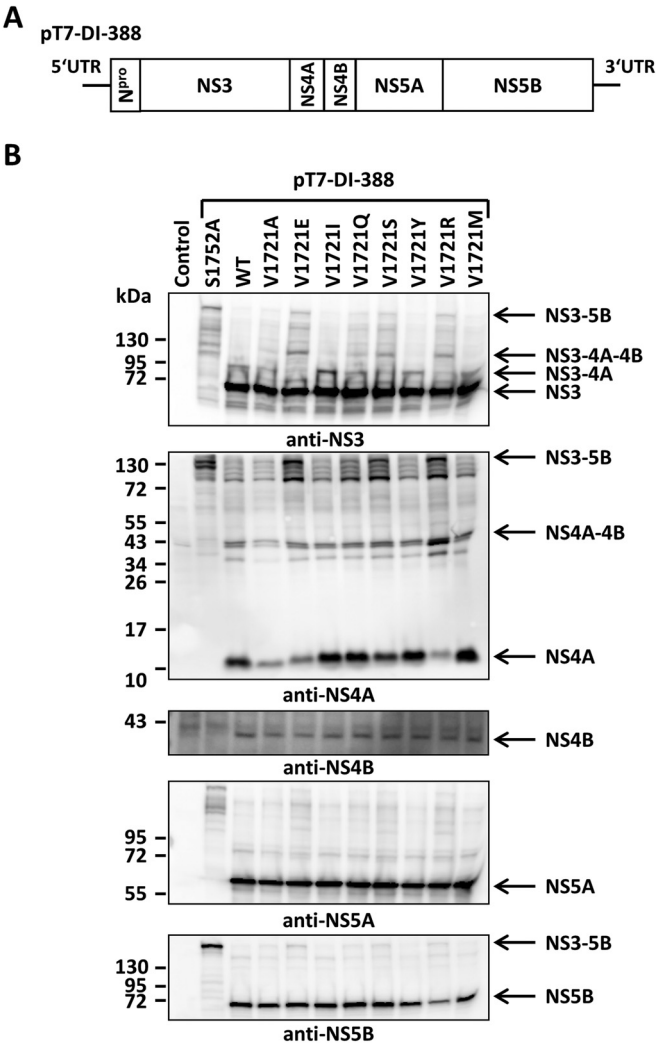

FIG 6 Amino acid permutations at position 1721 influence NS3 serine protease function during polyprotein processing. (A) Schematic drawing of pT7-DI-388. This construct encodes the proteins NS3-NS5B, representing the viral RNA replicase. The authentic N terminus of NS3 is generated by the autoprotease Npro. (B) Analysis of polyprotein processing by Western blot analysis. Huh7-T7 cells were infected with MVA-T7pol and subsequently transfected with 4 μg of the respective plasmid DNA. Protein expression was carried out overnight. Cells were lysed in 120 μl sample buffer. Twenty microliters of the cell lysate were separated by SDS-PAGE (NS3, NS4B, NS5A, and NS5B, 8% acrylamide; NS4A, 10% acrylamide), and proteins were visualized by Western blotting using protein-specific primary antibodies. Control, MVA-T7pol-infected Huh7-T7 cells; S1752A, inactivated NS3 protease, negative control; WT, wild-type (V1721); one representative experiment out of 3 replicates is shown. Polyprotein processing products are indicated on the right.

ruses regarding virion morphogenesis is the different uses of the proteins of the NS2-3-4A region. In the case of HCV, complete cleavage between NS2 and NS3 is believed to occur, and artificial separation of the NS2 and NS3 genes by an IRES element did not interfere with virion morphogenesis in cell culture (32, 33). In contrast, for pestiviruses, NS2-3 cleavage is temporally regulated throughout the course of infection, leading to an accumulation of uncleaved NS2-3 at later time points. A study in which NS2-3 cleavage was induced by a ubiquitin monomer inserted between NS2 and NS3 of BVDV strain NADL demonstrated an essential role for uncleaved NS2-3 for the production of infectious viruses. These investigations also revealed a critical role for NS4A in this process (15). An analogous approach using CSFV came to similar conclusions. In the latter study, *trans*-complementation studies provided convincing evidence that none of the enzymatic functions residing in NS2-3 are essential for virion morphogenesis (19). The authors also demonstrated that N-terminal truncations of NS2-3 disrupt its packaging function. Taken together, these data point to remarkable differences in the protein sets required for virion morphogenesis between the viruses of the genera *Pestivirus* and *Hepacivirus*.

In a recent study by Lattwein et al., a chimeric BVDV-1 genome was constructed encompassing the NS2-4B* region of cytopathogenic BVDV strain Osloss (34). The latter genome encodes a ubiquitin monomer between NS2 and NS3 due to a natural recombination event. Investigations using this chimeric genome demonstrated for the first time that it is possible to adapt pestiviruses to virion morphogenesis in the absence of uncleaved NS2-3. The molecular characterization of this virus derivative revealed that this chimera still requires NS2 for virion morphogenesis, since a C-terminal truncation of NS2 by 10 amino acids or a mutation in its putative structural Zn^{2+} binding site interfered with virion production (34). However, from this study it was not possible to delineate which of the individual amino acid differences between the NS2-4B* regions of the two parental strains are required to adapt for the absence of uncleaved NS2-3 or to compensate for the chimeric nature of this virus. This important issue is the focal point of the present study, where we characterized the individual amino acid contributions for the NS2-3-independent virion morphogenesis of a pestivirus. The major conclusion of this analysis is that only two amino acid exchanges, E1576V in NS2 and V1721A in NS3, are necessary and sufficient to allow efficient virion morphogenesis in the absence of uncleaved NS2-3 (Fig. 3). This surprising result shows that actually only minor changes in the NS2-3 region of the polyprotein are required to allow the adaptation of a pestivirus BVDV-1 to packaging requirements similar to those of HCV. Furthermore, we could demonstrate that in the context of strain NCP7, the mutation 2/RQ, previously identified by Lattwein et al. in the hydrophobic N-terminal region of NS2, was not required (34). Accordingly, this mutation most likely represents an adaptation to the chimeric nature of the used virus (Fig. 3).

TABLE 5 Functional analysis of amino acid permutations at position 1721 in NS3[a]

aa V1721 (NS3) change	aa characteristic(s)	RNA replication	Viral titer 48 h pe[b] ($TCID_{50}$/ml)
Alanine	Nonpolar/hydrophobic	+	5.0×10^5
Isoleucine	Nonpolar/hydrophobic	+	—
Methionine	Nonpolar/hydrophobic	+	—
Tyrosine	Polar/neutral	+	—
Glutamine	Polar/neutral	+	—
Serine	Polar/neutral	+	1.7×10^5
Glutamic acid	Acidic	−	ND
Arginine	Basic	−	ND

[a] Amino acids indicated were used to alter valine 1721 in the context of N7-2/EV-Ubi-3/VA. Data shown are from one representative experiment out of 3 independent experiments.
[b] A dash indicates no NS3-positive cells or infectious viruses were detected at 48 h pe. Virus derivatives with no detectable RNA replication were not analyzed for viral titers. ND, not determined.

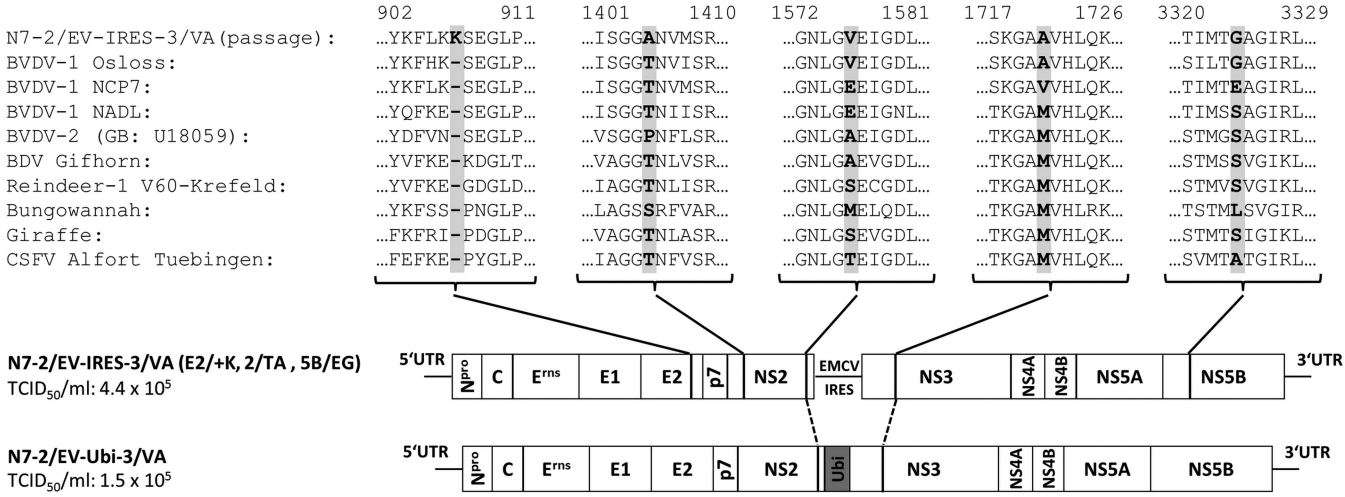

FIG 7 Alignment of different pestivirus strains at the amino acid positions which are critical for NS2-3-independent virion morphogenesis in monocistronic and bicistronic virus derivatives. Amino acid sequence of the passaged and biologically cloned virus derivative N7-2/EV-IRES-3/VA (passage) was compared to a selection of pestivirus sequences. Relevant amino acid positions are highlighted by boldfaced letters. Black lines mark the positions of the mutations in the newly generated derivatives N7-2/EV-IRES-3/VA (E2/+K, 2/TA, and 3/EG) and N7-2/EV-Ubi-3/VA. The virus titers indicated were determined 72 h pi (MOI, 0.1) (Fig. 3). Sequences with the following accession numbers were used: BVDV-1 Osloss, M96687; BVDV-1 NCP7 is identical to CP7-5A in the aligned regions (AF220247; BVDV-1 NADL, AJ133738; BVDV-2, U18059; BDV Gifhorn, KF925348; Reindeer-1 V60-Krefeld, AF144618; Bungowannah, EF100713; Giraffe, NC_003678; CSFV Alfort Tuebingen, J04358.

In the absence of structural data it remains unclear how the Glu-to-Val exchange at position 1576 located in the very C-terminal part of NS2 contributes to the restoration of virion morphogenesis. Our mutagenesis study revealed that at this position, Val or Tyr allowed for efficient virion production, while Ile or Met displayed a moderate ability to promote virion formation (Table 4). For mutants with Ala, Gln, Ser, or Arg at this position, no virion production was detectable (Table 4).

The C-terminal part of NS2 encompassing the cysteine protease domain is assumed to be located at the cytoplasmic side of the ER membrane. This assumption is based in part on the interaction of this domain with Jiv-cofactor fragments residing in the cytoplasm (21). Due to their hydrophobic characteristics, one can speculate that Val or Tyr at position 1576 supports protein-protein interactions between viral and/or cellular components of the packaging machinery.

For position 1721, located in the NS3-4A serine protease domain, it was observed that charged amino acids (Arg and Glu) abolished viral RNA replication (Fig. 5), which correlated with inefficient polyprotein processing but not with a complete loss of protease function (Fig. 6). This indicates that these mutant NS3 proteins generally are not misfolded, pointing to a more subtle defect in protein function. In contrast, most other NS3 mutants showed RNA replication comparable to that of the wild type (Fig. 5B and Table 5). Surprisingly, only the changes from Val to Ala or Ser allowed for efficient virion morphogenesis, indicating that specific requirements have to be fulfilled for this gain of function in NS3 (Table 5).

For HCV, a critical role of NS2 in orchestrating structural and nonstructural proteins during virion morphogenesis has been shown in several studies. Along these lines, HCV NS2 has been shown to interact either directly or indirectly with E1, E2, p7, NS3, NS4A, NS5A, and NS5B (44–48). Another study revealed interactions of NS2 with E1, E2, and p7, which are mediated by the transmembrane segments of the respective proteins (49). Similar studies for pestiviruses will significantly benefit from our identified gain-of-function mutants in NS2 and NS3. For the first time, highly similar packaging-competent and packaging-incompetent NS2/NS3 variants can be compared regarding viral assembly complex formation. Studies using those new tools also can address the question of which stage particle assembly or virion infectivity is stalled in the absence of uncleaved NS2-3.

Interestingly, in a bicistronic virus containing an EMCV IRES between the NS2 and NS3 genes, the situation turned out to be more complex. In this context, the two selected amino acid exchanges also were sufficient to allow virion morphogenesis, but the efficiency of infectious particle formation was notably decreased compared to that of the monocistronic virus derivative (Fig. 3C and D). Three additional adaptive mutations, in E2 (E2/+K), NS2 (2/TA), and NS5B (5B/EG), respectively, increased the virion morphogenesis efficiency of the bicistronic virus significantly (Fig. 3D). However, this occurred only when introduced in combination (data not shown). The fact that more adaptive mutations were required may reflect that functional protein-protein interactions are more efficiently established in the context of a polyprotein than with independently translated polypeptides.

In E2, an additional Lys residue was identified between amino acids 906 and 907. This amino acid position is located in the E2 ectodomain (50). Mutations increasing the positive charge of the surface of envelope proteins are common cell culture-adaptive mutations and were observed for E^{rns} of pestiviruses (51), glycoproteins of tick-borne encephalitis virus (TBEV) (52), picornaviruses (53, 54), alphaviruses (55, 56), and retroviruses (57, 58). This kind of mutation is thought to enhance the attachment step of the virus particle by binding to negatively charged glycosaminoglycans on the cell surface. Therefore, this mutation in E2 more likely improves the efficiency of virus attachment and uptake than being involved in the steps of particle assembly and virus release.

The function of NS2 mutation T1405A is hard to derive from the obtained data, since no structural data are available for pesti-

viral NS2. This amino acid is also located in the C-terminal cysteine protease domain of NS2; therefore, it is supposed to have a cytoplasmic location. The Thr-to-Ala exchange reduces the polarity; thus, it also may promote hydrophobic protein-protein interactions.

Finally, the mutation 5B/EG is localized in the N-terminal region of NS5B. In the Osloss genome, a glycine residue is encoded at this position (Fig. 7). The findings in this study are the first indication for an involvement of the N-terminal NS5B domain in virion morphogenesis. So far, only the C terminus of NS5B could be identified experimentally as being critical for infectious particle formation (16). An effect of the mutation 5B/EG on RNA replication efficiency has been excluded (Fig. 4). Accordingly, the effect on virus production more likely is due to a critical role of the NS5B N terminus in protein-protein interactions, which is further supported by the localization of E3324 on the protein surface (59).

Figure 7 shows an alignment of polyprotein fragments originating from different pestiviruses. This comparison illustrates that only the BVDV-1 strain Osloss has in NS2, NS3, and NS5B the amino acid residues required to support NS2-3-independent virion morphogenesis. This fact may explain why an analogous selection based on ncp BVDV-1 strain NCP7 with a Ubi insertion between NS2 and NS3 did not yield packaging-competent viruses (data not shown). Thus, the use of the Osloss strain with its unique properties and sequence turned out to be instrumental for the success of this approach.

Taken together, this study clearly shows that pestiviruses can be adapted to NS2-3-independent virion morphogenesis. The novel gain of function of cleaved NS2 and NS3 observed in this study by just two amino acid exchanges is intriguing. This fact is in line with the assumption that an ancestral virus already used this mechanism but lost it in the course of adapting to a new host/infection strategy. However, to finally unravel the underlying mechanism, structural data on NS2 and the NS3-4A protease complex will be of crucial importance.

ACKNOWLEDGMENTS

We especially thank S. Schwindt and M. Alexander for excellent technical assistance. We are grateful to E. J. Dubovi (Cornell University, Ithaca, NY) for antibody 8.12.7; T. Rümenapf and B. Lamp (University of Veterinary Medicine, Vienna, Austria) for providing antibodies GH4A1 (4B7), GL4B1, GLBVD5A1 (11C), and GLBVD5B1 (9A); S. Lemon (UNC, Chapel Hill, NC) for providing us with the Huh7-T7 cell line; and G. Sutter (LMU, Munich, Germany) for the MVA-T7pol vaccinia virus stock. We also thank Olaf Isken for helpful discussions.

This work was supported by intramural funding from the University of Lübeck.

REFERENCES

1. **Pletnev A, Gould E, Heinz FX, Meyers G, Thiel H-J, Bukh J, Stiasny K, Collett MS, Becher P, Simmonds P, Rice CM, Monath TP.** 2011. Flaviviridae, p 1003–1020. *In* King AMQ, Adams MJ, Carstens EB, Lefkowitz EJ (ed), Virus taxonomy. Ninth report of the International Committee on Taxonomy of Viruses. Elsevier Inc., Oxford, United Kingdom.
2. **Stapleton JT, Foung S, Muerhoff AS, Bukh J, Simmonds P.** 2011. The GB viruses: a review and proposed classification of GBV-A, GBV-C (HGV), and GBV-D in genus Pegivirus within the family Flaviviridae. J Gen Virol **92:**233–246. http://dx.doi.org/10.1099/vir.0.027490-0.
3. **Tautz N, Tews BA, Meyers G.** 2015. The molecular biology of pestiviruses. Adv Virus Res **93:**47–160. http://dx.doi.org/10.1016/bs.aivir.2015.03.002.
4. **Lindenbach BD, Murray CL, Thiel HJ, Rice CM.** 2013. *Flaviviridae*, p 712–746. *In* Knipe DM, Howley PM (ed), Fields virology, 6th ed, vol 1. Lippincott Williams & Wilkins, Philadelphia, PA.
5. **Bintintan I, Meyers G.** 2010. A new type of signal peptidase cleavage site identified in an RNA virus polyprotein. J Biol Chem **285:**8572–8584. http://dx.doi.org/10.1074/jbc.M109.083394.
6. **Lackner T, Müller A, Pankraz A, Becher P, Thiel H-J, Gorbalenya AE, Tautz N.** 2004. Temporal modulation of an autoprotease is crucial for replication and pathogenicity of an RNA virus. J Virol **78:**10765–10775. http://dx.doi.org/10.1128/JVI.78.19.10765-10775.2004.
7. **Tamura JK, Warrener P, Collett MS.** 1993. RNA-stimulated NTPase activity associated with the p80 protein of the pestivirus bovine viral diarrhea virus. Virology **193:**1–10. http://dx.doi.org/10.1006/viro.1993.1097.
8. **Warrener P, Collett MS.** 1995. Pestivirus NS3 (p80) protein possesses RNA helicase activity. J Virol **69:**1720–1726.
9. **Wiskerchen M, Collett MS.** 1991. Pestivirus gene expression: protein p80 of bovine viral diarrhea virus is a proteinase involved in polyprotein processing. Virology **184:**341–350. http://dx.doi.org/10.1016/0042-6822(91)90850-B.
10. **Tortorici MA, Duquerroy S, Kwok J, Vonrhein C, Perez J, Lamp B, Bricogne G, Rümenapf T, Vachette P, Rey FA.** 2015. X-ray structure of the pestivirus NS3 helicase and its conformation in solution. J Virol **89:**4356–4371. http://dx.doi.org/10.1128/JVI.03165-14.
11. **Tautz N, Kaiser A, Thiel HJ.** 2000. NS3 serine protease of bovine viral diarrhea virus: characterization of active site residues, NS4A cofactor domain, and protease-cofactor interactions. Virology **273:**351–363. http://dx.doi.org/10.1006/viro.2000.0425.
12. **Xu J, Mendez E, Caron PR, Lin C, Murcko MA, Collett MS, Rice CM.** 1997. Bovine viral diarrhea virus NS3 serine proteinase: polyprotein cleavage sites, cofactor requirements, and molecular model of an enzyme essential for pestivirus replication. J Virol **71:**5312–5322.
13. **Behrens SE, Grassmann CW, Thiel HJ, Meyers G, Tautz N.** 1998. Characterization of an autonomous subgenomic pestivirus RNA replicon. J Virol **72:**2364–2372.
14. **Murray CL, Jones CT, Rice CM.** 2008. Architects of assembly: roles of Flaviviridae non-structural proteins in virion morphogenesis. Nat Rev Microbiol **6:**699–708. http://dx.doi.org/10.1038/nrmicro1928.
15. **Agapov EV, Murray CL, Frolov I, Qu L, Myers TM, Rice CM.** 2004. Uncleaved NS2-3 is required for production of infectious bovine viral diarrhea virus. J Virol **78:**2414–2425. http://dx.doi.org/10.1128/JVI.78.5.2414-2425.2004.
16. **Ansari IH, Chen L-M, Liang D, Gil LH, Zhong W, Donis RO.** 2004. Involvement of a bovine viral diarrhea virus NS5B locus in virion assembly. J Virol **78:**9612–9623. http://dx.doi.org/10.1128/JVI.78.18.9612-9623.2004.
17. **Harada T, Tautz N, Thiel HJ.** 2000. E2-p7 region of the bovine viral diarrhea virus polyprotein: processing and functional studies. J Virol **74:**9498–9506. http://dx.doi.org/10.1128/JVI.74.20.9498-9506.2000.
18. **Isken O, Langerwisch U, Schönherr R, Lamp B, Schröder K, Duden R, Rümenapf TH, Tautz N.** 2014. Functional characterization of bovine viral diarrhea virus nonstructural protein 5A by reverse genetic analysis and live cell imaging. J Virol **88:**82–98. http://dx.doi.org/10.1128/JVI.01957-13.
19. **Moulin HR, Seuberlich T, Bauhofer O, Bennett LC, Tratschin J-D, Hofmann MA, Ruggli N.** 2007. Nonstructural proteins NS2-3 and NS4A of classical swine fever virus: essential features for infectious particle formation. Virology **365:**376–389. http://dx.doi.org/10.1016/j.virol.2007.03.056.
20. **Han Q, Manna D, Belton K, Cole R, Konan KV.** 2013. Modulation of hepatitis C virus genome encapsidation by nonstructural protein 4B. J Virol **87:**7409–7422. http://dx.doi.org/10.1128/JVI.03523-12.
21. **Lackner T, Müller A, König M, Thiel H-J, Tautz N.** 2005. Persistence of bovine viral diarrhea virus is determined by a cellular cofactor of a viral autoprotease. J Virol **79:**9746–9755. http://dx.doi.org/10.1128/JVI.79.15.9746-9755.2005.
22. **Lackner T, Thiel H-J, Tautz N.** 2006. Dissection of a viral autoprotease elucidates a function of a cellular chaperone in proteolysis. Proc Natl Acad Sci U S A **103:**1510–1515. http://dx.doi.org/10.1073/pnas.0508247103.
23. **Becher P, Tautz N.** 2011. RNA recombination in pestiviruses: Cellular RNA sequences in viral genomes highlight the role of host factors for viral persistence and lethal disease. RNA Biol **8:**216–224. http://dx.doi.org/10.4161/rna.8.2.14514.
24. **Brownlie J, Clarke MC, Howard CJ.** 1984. Experimental production of fatal mucosal disease in cattle. Vet Rec **114:**535–536. http://dx.doi.org/10.1136/vr.114.22.535.

25. **Kümmerer BM, Tautz N, Becher P, Thiel H-J, Meyers G.** 2000. The genetic basis for cytopathogenicity of pestiviruses. Vet Microbiol **77:**117–128. http://dx.doi.org/10.1016/S0378-1135(00)00268-6.
26. **Liess B, Orban S, Frey HR, Trautwein G, Wiefel W, Blindow H.** 1984. Studies on transplacental transmissibility of a bovine virus diarrhoea (BVD) vaccine virus in cattle. II. Inoculation of pregnant cows without detectable neutralizing antibodies to BVD virus 90-229 days before parturition (51st to 190th day of gestation). Zentralbl Veterinarmed B **31:**669–681.
27. **Gamlen T, Richards KH, Mankouri J, Hudson L, McCauley J, Harris M, Macdonald A.** 2010. Expression of the NS3 protease of cytopathogenic bovine viral diarrhea virus results in the induction of apoptosis but does not block activation of the beta interferon promoter. J Gen Virol **91:**133–144. http://dx.doi.org/10.1099/vir.0.016170-0.
28. **Grummer B, Bendfeldt S, Greiser-Wilke I.** 2002. Apoptosis inhibitors delay the cytopathic effect of bovine viral diarrhoea virus (BVDV). J Vet Med B Infect Dis Vet Public Health **49:**298–303. http://dx.doi.org/10.1046/j.1439-0450.2002.00573.x.
29. **Hoff HS, Donis RO.** 1997. Induction of apoptosis and cleavage of poly(ADP-ribose) polymerase by cytopathic bovine viral diarrhea virus infection. Virus Res **49:**101–113. http://dx.doi.org/10.1016/S0168-1702(97)01460-3.
30. **Vassilev VB, Donis RO.** 2000. Bovine viral diarrhea virus induced apoptosis correlates with increased intracellular viral RNA accumulation. Virus Res **69:**95–107. http://dx.doi.org/10.1016/S0168-1702(00)00176-3.
31. **Zhang G, Aldridge S, Clarke MC, McCauley JW.** 1996. Cell death induced by cytopathic bovine viral diarrhoea virus is mediated by apoptosis. J Gen Virol **77**(Part 8)**:**1677–1681. http://dx.doi.org/10.1099/0022-1317-77-8-1677.
32. **Jirasko V, Montserret R, Appel N, Janvier A, Eustachi L, Brohm C, Steinmann E, Pietschmann T, Penin F, Bartenschlager R.** 2008. Structural and functional characterization of nonstructural protein 2 for its role in hepatitis C virus assembly. J Biol Chem **283:**28546–28562. http://dx.doi.org/10.1074/jbc.M803981200.
33. **Jones CT, Murray CL, Eastman DK, Tassello J, Rice CM.** 2007. Hepatitis C virus p7 and NS2 proteins are essential for production of infectious virus. J Virol **81:**8374–8383. http://dx.doi.org/10.1128/JVI.00690-07.
34. **Lattwein E, Klemens O, Schwindt S, Becher P, Tautz N.** 2012. Pestivirus virion morphogenesis in the absence of uncleaved nonstructural protein 2-3. J Virol **86:**427–437. http://dx.doi.org/10.1128/JVI.06133-11.
35. **Corapi W, Donis R, Dubovi E.** 1988. Monoclonal antibody analyses of cytopathic and noncytopathic viruses from fatal bovine viral diarrhea virus infections. J Virol **62:**2823–2827.
36. **De Moerlooze L, Lecomte C, Brown-Shimmer S, Schmetz D, Guiot C, Vandenbergh D, Allaer D, Rossius M, Chappuis G, Dina D.** 1993. Nucleotide sequence of the bovine viral diarrhoea virus Osloss strain: comparison with related viruses and identification of specific DNA probes in the 5′ untranslated region. J Gen Virol **74**(Part 7)**:**1433–1438. http://dx.doi.org/10.1099/0022-1317-74-7-1433.
37. **Sutter G, Ohlmann M, Erfle V.** 1995. Non-replicating vaccinia vector efficiently expresses bacteriophage T7 RNA polymerase. FEBS Lett **371:**9–12. http://dx.doi.org/10.1016/0014-5793(95)00843-X.
38. **Corapi WV, Donis RO, Dubovi EJ.** 1990. Characterization of a panel of monoclonal antibodies and their use in the study of the antigenic diversity of bovine viral diarrhea virus. Am J Vet Res **51:**1388–1394.
39. **Meyers G, Tautz N, Becher P, Thiel HJ, Kümmerer BM.** 1996. Recovery of cytopathogenic and noncytopathogenic bovine viral diarrhea viruses from cDNA constructs. J Virol **70:**8606–8613.
40. **Pankraz A, Thiel H-J, Becher P.** 2005. Essential and nonessential elements in the 3′ nontranslated region of bovine viral diarrhea virus. J Virol **79:**9119–9127. http://dx.doi.org/10.1128/JVI.79.14.9119-9127.2005.
41. **Schultz DE, Honda M, Whetter LE, McKnight KL, Lemon SM.** 1996. Mutations within the 5′ nontranslated RNA of cell culture-adapted hepatitis A virus which enhance cap-independent translation in cultured African green monkey kidney cells. J Virol **70:**1041–1049.
42. **Tautz N, Harada T, Kaiser A, Rinck G, Behrens S, Thiel HJ.** 1999. Establishment and characterization of cytopathogenic and noncytopathogenic pestivirus replicons. J Virol **73:**9422–9432.
43. **Schägger H, von Jagow G.** 1987. Tricine-sodium dodecyl sulfate-polyacrylamide gel electrophoresis for the separation of proteins in the range from 1 to 100 kDa. Anal Biochem **166:**368–379. http://dx.doi.org/10.1016/0003-2697(87)90587-2.
44. **Dimitrova M, Imbert I, Kieny MP, Schuster C.** 2003. Protein-protein interactions between hepatitis C virus nonstructural proteins. J Virol **77:**5401–5414. http://dx.doi.org/10.1128/JVI.77.9.5401-5414.2003.
45. **Gouklani H, Bull RA, Beyer C, Coulibaly F, Gowans EJ, Drummer HE, Netter HJ, White PA, Haqshenas G.** 2012. Hepatitis C virus NS5B is involved in virus morphogenesis. J Virol **86:**5080–5088. http://dx.doi.org/10.1128/JVI.07089-11.
46. **Gouklani H, Beyer C, Drummer H, Gowans EJ, Netter HJ, Haqshenas G.** 2013. Identification of specific regions in hepatitis C virus core, NS2 and NS5A that genetically interact with p7 and co-ordinate infectious virus production. J Viral Hepat **20:**e66–71. http://dx.doi.org/10.1111/jvh.12004.
47. **Ma Y, Anantpadma M, Timpe JM, Shanmugam S, Singh SM, Lemon SM, Yi M.** 2011. Hepatitis C virus NS2 protein serves as a scaffold for virus assembly by interacting with both structural and nonstructural proteins. J Virol **85:**86–97. http://dx.doi.org/10.1128/JVI.01070-10.
48. **Yi M, Ma Y, Yates J, Lemon SM.** 2007. Compensatory mutations in E1, p7, NS2, and NS3 enhance yields of cell culture-infectious intergenotypic chimeric hepatitis C virus. J Virol **81:**629–638. http://dx.doi.org/10.1128/JVI.01890-06.
49. **Jirasko V, Montserret R, Lee JY, Gouttenoire J, Moradpour D, Penin F, Bartenschlager R.** 2010. Structural and functional studies of nonstructural protein 2 of the hepatitis C virus reveal its key role as organizer of virion assembly. PLoS Pathog **6:**e1001233. http://dx.doi.org/10.1371/journal.ppat.1001233.
50. **El Omari K, Iourin O, Harlos K, Grimes JM, Stuart DI.** 2013. Structure of a pestivirus envelope glycoprotein E2 clarifies its role in cell entry. Cell Rep **3:**30–35. http://dx.doi.org/10.1016/j.celrep.2012.12.001.
51. **Hulst MM, Moormann RJ.** 2001. Erns protein of pestiviruses. Methods Enzymol **342:**431–440. http://dx.doi.org/10.1016/S0076-6879(01)42564-X.
52. **Mandl CW, Kroschewski H, Allison SL, Kofler R, Holzmann H, Meixner T, Heinz FX.** 2001. Adaptation of tick-borne encephalitis virus to BHK-21 cells results in the formation of multiple heparan sulfate binding sites in the envelope protein and attenuation in vivo. J Virol **75:**5627–5637. http://dx.doi.org/10.1128/JVI.75.12.5627-5637.2001.
53. **Escarmís C, Carrillo EC, Ferrer M, Arriaza JF, Lopez N, Tami C, Verdaguer N, Domingo E, Franze-Fernández MT.** 1998. Rapid selection in modified BHK-21 cells of a foot-and-mouth disease virus variant showing alterations in cell tropism. J Virol **72:**10171–10179.
54. **Sa-Carvalho D, Rieder E, Baxt B, Rodarte R, Tanuri A, Mason PW.** 1997. Tissue culture adaptation of foot-and-mouth disease virus selects viruses that bind to heparin and are attenuated in cattle. J Virol **71:**5115–5123.
55. **Bernard KA, Klimstra WB, Johnston RE.** 2000. Mutations in the E2 glycoprotein of Venezuelan equine encephalitis virus confer heparan sulfate interaction, low morbidity, and rapid clearance from blood of mice. Virology **276:**93–103. http://dx.doi.org/10.1006/viro.2000.0546.
56. **Klimstra WB, Ryman KD, Johnston RE.** 1998. Adaptation of Sindbis virus to BHK cells selects for use of heparan sulfate as an attachment receptor. J Virol **72:**7357–7366.
57. **Moulard M, Lortat-Jacob H, Mondor I, Roca G, Wyatt R, Sodroski J, Zhao L, Olson W, Kwong PD, Sattentau QJ.** 2000. Selective interactions of polyanions with basic surfaces on human immunodeficiency virus type 1 gp120. J Virol **74:**1948–1960. http://dx.doi.org/10.1128/JVI.74.4.1948-1960.2000.
58. **Patel M, Yanagishita M, Roderiquez G, Bou-Habib DC, Oravecz T, Hascall VC, Norcross MA.** 1993. Cell-surface heparan sulfate proteoglycan mediates HIV-1 infection of T-cell lines. AIDS Res Hum Retroviruses **9:**167–174. http://dx.doi.org/10.1089/aid.1993.9.167.
59. **Choi KH, Gallei A, Becher P, Rossmann MG.** 2006. The structure of bovine viral diarrhea virus RNA-dependent RNA polymerase and its amino-terminal domain. Structure **14:**1107–1113. http://dx.doi.org/10.1016/j.str.2006.05.020.